Synthesis of Tire Equations for Use in Shimmy and Other Dynamic Studies

L. C. Rogers* and H. K. Brewer†
Wright-Patterson Air Force Base, Ohio

A system of transfer functions relating the cornering force and aligning torque of a rolling pneumatic tire to its yaw angle and lateral displacement are developed from experimental and theoretical frequency response curves. These transfer functions consist of ratios of polynomials in the Laplacian variable s, which lead to a system of linear constant coefficient differential equations. The resulting equations have the advantage of both simplicity and accuracy and are ideally suited for use in dynamical analysis such as the study of wheel shimmy phenomena. These differential equations, along with the corresponding experimental frequency response curves, are compared with those derived from the widely used Moreland tire theory. This comparison reveals a number of inadequacies in the Moreland theory.

Introduction

RELATIONS expressing tire forces in terms of the wheel yaw angle and lateral displacement are required in various studies in aircraft and ground vehicle dynamics, including the analysis of wheel shimmy. There are at present numerous tire theories[1–6] available for calculating these necessary relationships. Unfortunately, from a dynamicist's point of view, these theories are not totally satisfactory. On the one hand, comparatively simple models such as that of Moreland,[1] while being of a form convenient for dynamic analysis, suffer from lack of accuracy in characterizing the tire behavior (see Appendix). Conversely, the more accurate theories such as that of Pacejka,[6] are complicated to the point of making them extremely cumbersome for direct use in the analysis of dynamical systems. Clearly, an immediate engineering need exists for a practical yet accurate method of representing transient tire forces.[13] The development of such a method is the subject of the present paper.

The technique to be described here makes direct use of experimental tire data in a frequency response format. This data along with principles from feedback and control systems theory (Bode Analysis) is utilized to develop a set of transfer functions which relate the tire force and moment response to variations in the wheel coordinates. Once these transfer functions are known, a corresponding system of differential equations can be written. It is known that if the tire behaves linearly and the frequency response is represented for all frequencies, then the transient condition is also covered, i.e., the equations are valid for arbitrary motions of the wheel.

The differential equations, thus, developed are especially convenient for use in dynamic analysis or simulation studies since they are of the linear constant efficient type. They become part of a set of equations, the rest of which may be nonlinear as necessary to represent the system under analysis.

Theoretical Considerations

It is well known that a pneumatic tire has the ability to roll without sliding, even though it may possess a velocity component normal to its wheel plane. Such motion is characterized by the presence of a slip angle α. This quantity is defined as the angle between the wheel plane and the total velocity vector of the wheel center. The formation of a slip angle may result from either of two fundamental motions, i.e., pure yaw or pure sideslip. A tire rolls in pure yaw when only the yaw angle ψ is allowed to vary and the lateral displacement y is held at zero (Fig. 1a). Conversely, in pure sideslip, the lateral displacement varies while the yaw angle is zero (Fig. 1b). In the general case, as on a moving vehicle, both motions occur simultaneously (Fig. 1c).

When a tire rolls with a slip angle it is constrained to undergo lateral deformation. For simplicity this deformation is often characterized by the lateral distortion of the tire equatorial line. The effect of this distortion is to set up a system of elastic restoring forces between the tire and wheel. The net resultant of these distributed forces is a force F acting normal to the wheel plane and a moment M acting about the vertical wheel axis. These quantities are known as the cornering force and aligning torque, respectively.

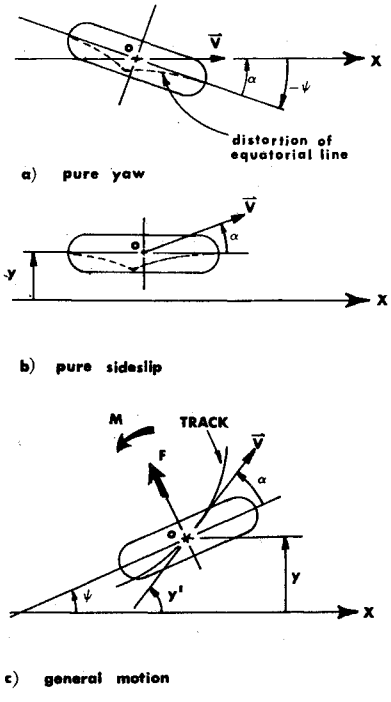

Fig. 1 Component motion of a pneumatic tire.

Received December 4, 1970; revision received April 12, 1971. The authors wish to express their appreciation to the B. F. Goodrich Research Center for providing the experimental frequency response tire data used in this study. This paper may be reproduced for purposes of the U.S. Government.

* Aerospace Engineer, Design Criteria Branch, Structures Division, Air Force Flight Dynamics Laboratory.

† Research Engineer, Mechanical Branch, Vehicle Equipment Division, Air Force Flight Dynamics Laboratory.

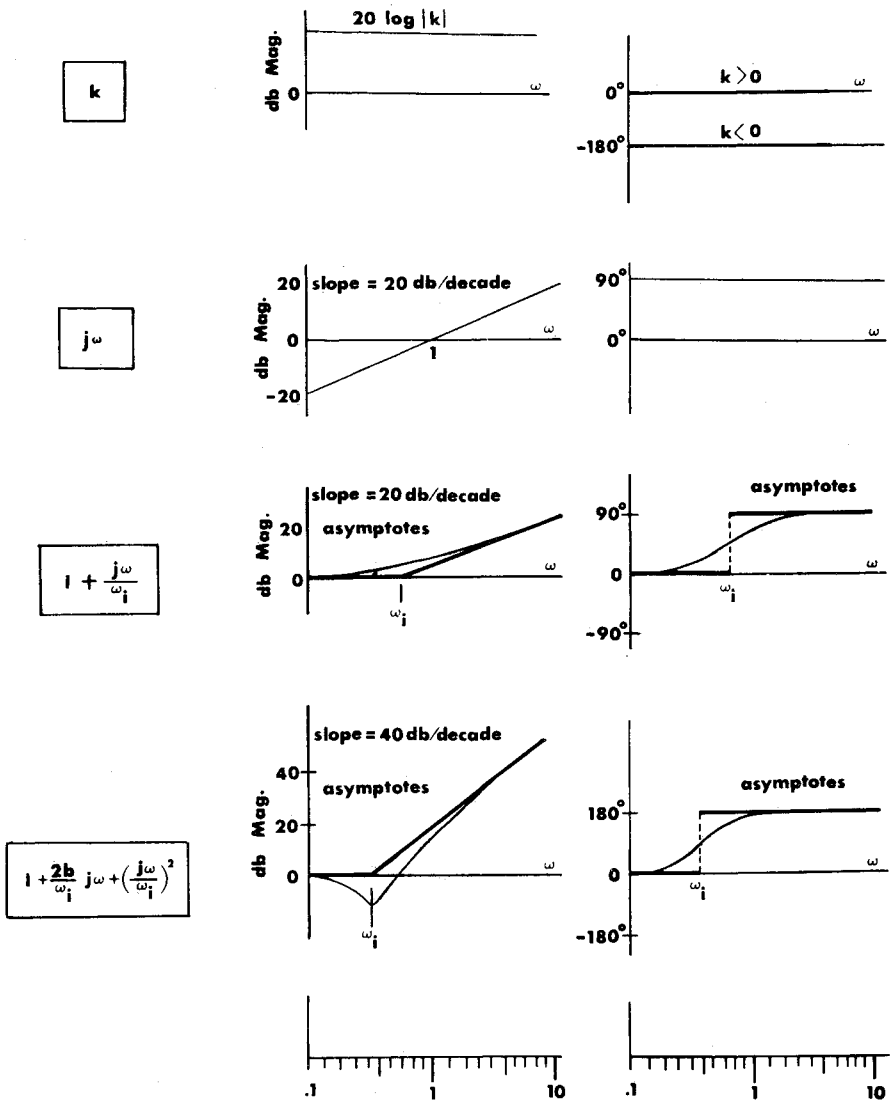

Fig. 2 Bode plots of typical polynomial factors.

A tire rolling at a slip angle is said to be in quasi-steady state when neither the yaw angle nor the lateral velocity vary with time. Under these conditions, the lateral distortion of the equatorial line with respect to the wheel is the same for both pure yaw and pure sideslip, provided the slip angles are also equal. It follows, in the quasi-steady state, that for pure yaw or pure sideslip the cornering force and aligning torque will also be equal. This of course is not true in the general nonsteady-state condition.[3]

Assume for the present that the differential equations which describe the tire behavior are of the general form

$$\phi + a\phi' + b\phi'' = k(\eta + c\eta' + d\eta'') \tag{1}$$

where a,b,c,d, and k are constants and primes denote differentiation with respect to the independent variable. In this equation for example, ϕ might represent the tire aligning torque and η the lateral displacement of the wheel, both as functions of the forward position coordinate x. Taking the Laplace transform of Eq. (1), and setting all initial values of ϕ and η and their first derivatives equal to zero results in

$$(1 + as + bs^2)\bar{\phi}(s) = k(1 + cs + ds^2)\bar{\eta}(s) \tag{2}$$

where barred quantities denote transformed variables. The transfer function $G_{\phi\eta}(s)$ associated with Eq. (1) is defined as the ratio of the Laplace transform of the output $\bar{\phi}(s)$ to that of the input $\bar{\eta}(s)$

$$G_{\phi\eta}(s) = \bar{\phi}(s)/\bar{\eta}(s) = k(1 + cs + ds^2)/(1 + as + bs^2) \tag{3}$$

If now the system described by Eq. (1) is subjected to a sinusoidal input

$$\eta = \eta_0 \sin(\omega x) \tag{4}$$

then after transients die out, the steady-state response will be

$$\phi(x) = \eta_0 |G_{\phi\eta}(j\omega)| \sin(\omega x - \theta) \tag{5}$$

where $|G_{\phi\eta}(jw)|$ and θ are the magnitude and argument, respectively of the complex number $G_{\phi\eta}(j\omega)$ which represents the system frequency response. The function $G_{\phi\eta}(j\omega)$ is determined from Eq. (3) by replacing the Laplacian variable s with $j\omega$.

The previous development briefly illustrates the procedure for determining the transfer function and the frequency response from the basic differential equation. It is clear that if this equation is of the linear constant coefficient type, then $G_{\phi\eta}(s)$ will be a rational algebraic function consisting of a ratio of polynomials in s. The object here, however, is the reverse operation, i.e., to synthesize the governing differential equation from an experimentally determined frequency response curve. The technique of Bode plots provides a very useful tool for this purpose.

The Bode plot of an arbitrary frequency response function $G_{\gamma\beta}(j\omega)|$ consists of two separate graphs: the magnitude $|G_{\gamma\beta}(j\omega)|$ and the phase angle arg $G_{\gamma\beta}(j\omega)$. Typically, both the magnitude in db units, called the "log magnitude," and the phase angle in degrees, are plotted vs frequency on a logarithmic scale. The log magnitude, denoted by Lm is

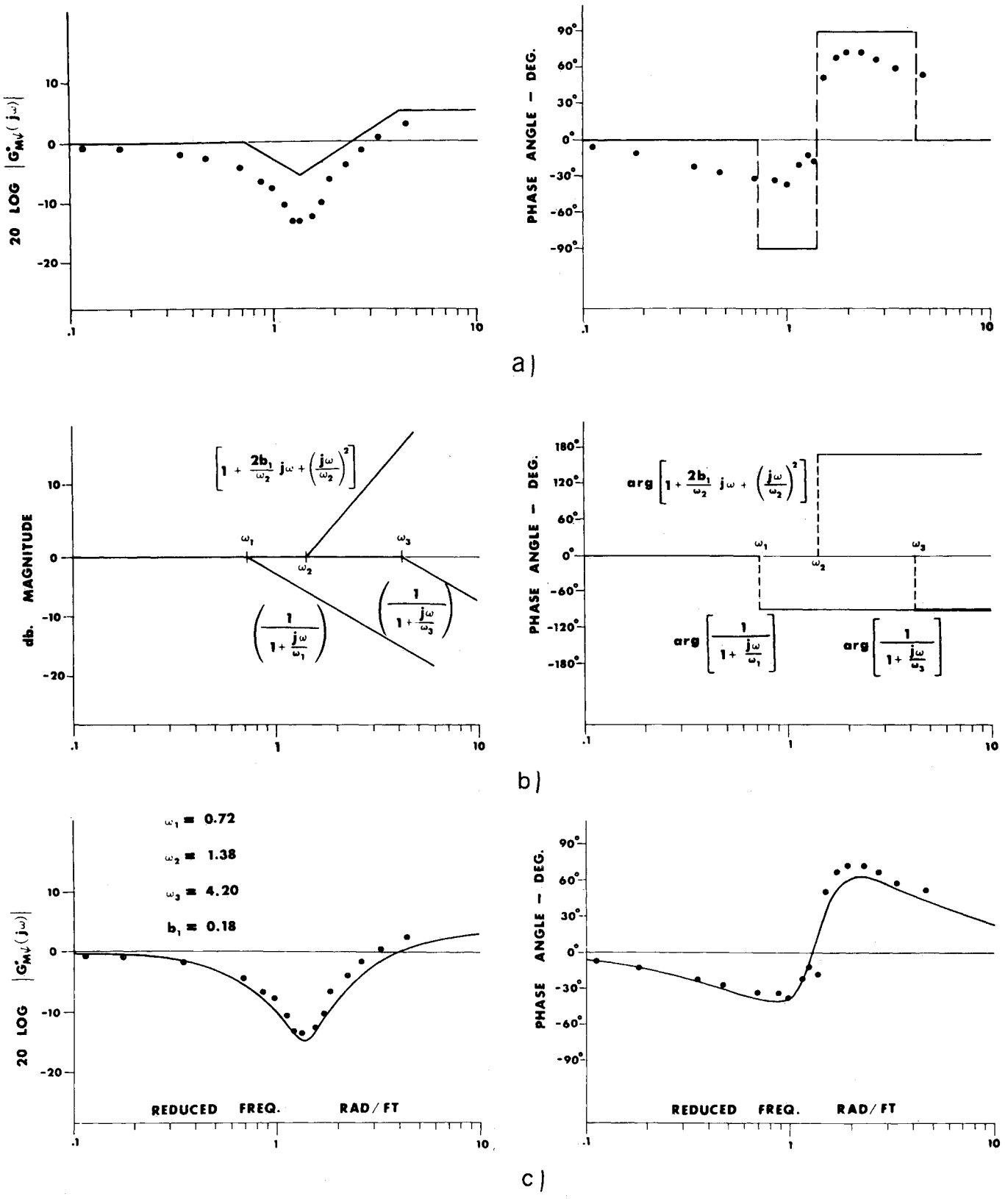

Fig. 3 Tire aligning torque frequency response under cyclic yaw.

defined as

$$LmG\gamma(j\omega) \equiv 20 \log_{10}|G_{\gamma\beta}(j\omega)| \qquad (6)$$

The use of logarithmic scales leads to a considerable simplification in the construction and interpretation of the plots. This is particularly true when $G_{\gamma\beta}(j\omega)$ consists of products and ratios of factored terms. In this case, the total or composite Bode magnitude plot is obtained by simply adding or substracting those of the individual terms. The same rule applied to the Bode phase angle plots according to theorems of complex algebra.

The terms most often encountered in the functions $G_{\gamma\beta}(j\omega)$ are the polynomials of various degrees in $j\omega$. Their Bode magnitude and phase angle plots have been systematically tabulated in standard reference works such as D'Azzo and Houpis. These plots form the basis of approximating a

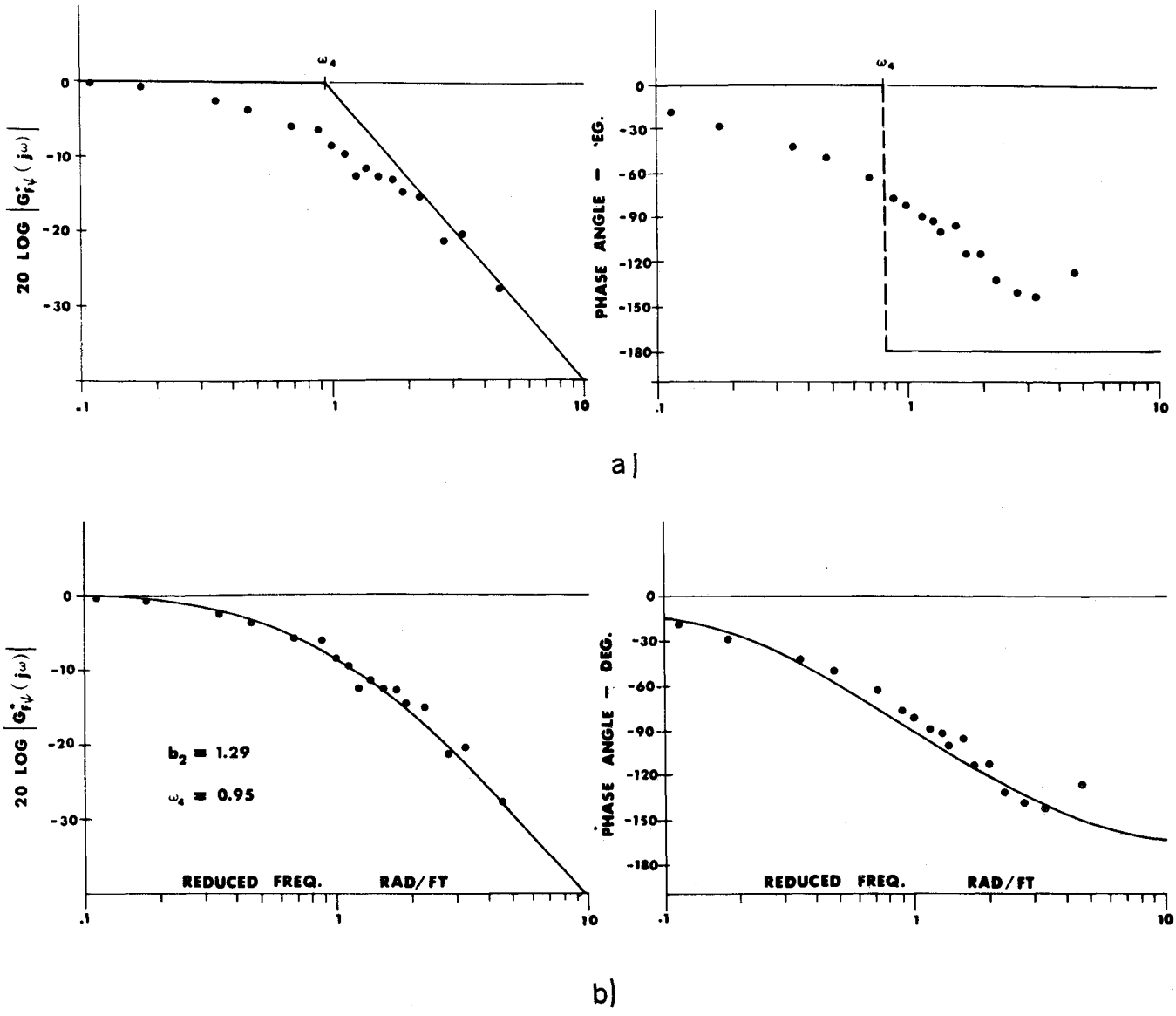

Fig. 4 Tire cornering force frequency response under cyclic yaw.

given experimental frequency response curve in terms of factored polynomials. A list of typical factors, together with plots of their low-frequency and high-frequency asymptotes is contained in Fig. 2. The corresponding plots of the reciprocal terms are obtained by simply reflecting the given curves about the ω axis. The abscissa in these plots is the frequency ω plotted on a log scale as indicated at the bottom of Fig. 2.

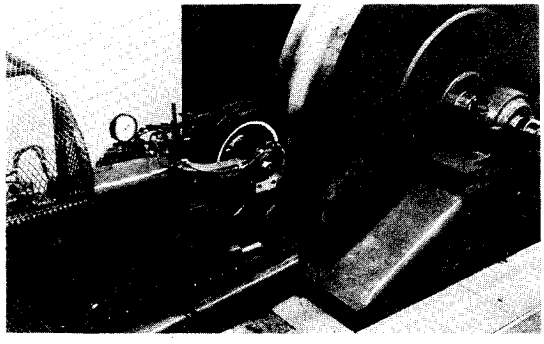

Fig. 5 Cyclic yaw tire test machine.[9]

Synthesis of Tire Frequency Response Functions

The technique of approximating the tire frequency response using Bode plots is best illustrated by a specific case. Consider the experimental response data shown in Fig. 3a for a tire undergoing sinusoidal variations in yaw angle. In these graphs, the magnitude of the aligning torque frequency response and its phase angle are plotted as functions of the frequency ω. This ω, in units of rad/ft, is the so called "path" or "reduced" angular frequency which is related to the cyclic time frequency f_t, in units of cps, according to

$$\omega = 2\pi f_t / V_x \tag{7}$$

where V_x is the forward velocity. The magnitude of the response has been normalized by dividing it by its value at zero frequency, i.e.,

$$|G_{M\psi}{}^*(j\omega)| = |G_{M\psi}(j\omega)|/G_{M\psi}(0) \tag{8}$$

To synthesize the frequency response in terms of polynomials, one first crudely approximates the magnitude curve with straight line segments as shown in Fig. 3a. Each segment must have a slope of $\pm$ 20n db/decade, where n is a positive integer. Simultaneously, the phase angle curve is approximated by line segments whose values are integer multiples of 90°. The straight line approximation of Fig. 3a can

obviously be achieved by the superposition of the three curves shown in Fig. 3b. Consulting the tabulation of polynomial factors in Fig. 2 it is seen that these line segments correspond to the asymptotes of the terms $[1 + (j\omega/\omega_1)]^{-1}$, $[1 + (2b_1/\omega_2)j\omega + (j\omega/\omega_2)^2]$, $[1 + (j\omega/\omega_3)^{-1}]$. The intersections of the asymptotic lines determine the corner frequencies ω_1,ω_2, and ω_3. The parameters $\omega_1,\omega_2,\omega_3$, and b_1 are varied to obtain the best fit of the data. Thus, the resulting expression for the aligning torque frequency response is

$$G_{M\psi}(j\omega) = G_{M\psi}(0)G_{M\psi}{}^*(j\omega) = G_{M\psi}(0)[1 + (2b_1/\omega_2)j\omega + (j\omega/\omega_2)^2]/[1 + (j\omega/\omega_1)][1 + (j\omega/\omega_3)] \quad (9)$$

A comparison of the experimental frequency response and its approximate representation according to Eq. (9) is given in Fig. 3c.

The cornering force frequency response is treated in a similar fashion. Referring to Fig. 4a, it is seen that experimental response can be roughly approximated by the asymptotes of the single term

$$1/[1 + (2b_2/\omega_4)j\omega + (j\omega/\omega_4)^2]$$

Thus, the cornering force frequency response is given by

$$G_{F\psi}(j\omega) = G_{F\psi}(0)G_{F\psi}{}^*(j\omega) = G_{F\psi}(0)/[1 + (2b_2/\omega_4)j\omega + (j\omega/\omega_4)^2] \quad (10a)$$

where again $G_{F\psi}(0)$ is the normalizing response at zero frequency and ω_4 and b_2 are parameters to be determined for a best fit of the data.

In the specific case of Fig. 4, since the value of b_2 is larger than unity, the denominator of Eq. (10a) can be expressed as two first-order terms of the form

$$G_{F\psi}(j\omega) = G_{F\psi}(0)/(1 + j\omega/\omega_a)(1 + j\omega/\omega_b) \quad (10b)$$

where $\omega_a = 0.45$ and $\omega_b = 2.00$.

The transfer functions corresponding to Eqs. (9) and (10a) are obtained by replacing $j\omega$ in these expressions with the Laplacian variable s. Clearly, these will be similar in form to Eq. (3).

$$G_{M\psi}(s) = G_{M\psi}(0)[1 + (2b_1/\omega_2)s + (s/\omega_2)^2]/(1 + s/\omega_1)(1 + s/\omega_3) \quad (11)$$

$$G_{F\psi}(s) = G_{F\psi}(0)/[1 + (2b_2/\omega_4)s + (s/\omega_4)^2] \quad (12)$$

Although the experimental frequency response data used in these calculations are for an automotive type tire, the indications are that it is characteristic of pneumatic tires in general. These data were generated on the tire test dynamometer shown in Fig. 5. Essentially this machine consists of a horizontal carriage which loads the tire against a rotating steel drum. The carriage is capable of subjecting the tire to a sinusoidal angular motion (yaw) about its horizontal axis, while simultaneous measurements are made of the cornering force and aligning torque. These measurements correspond to the steady-state response of Eq. (5). For a given time cyclic frequency of oscillation, 1 cps in this case, the wheel speed is varied so as to provide a complete range of reduced frequencies in accordance with Eq. (7). Details of this test machine are given in Ref. 9.

The transfer functions relating the cornering force and aligning torque to the lateral displacement are determined by repeating the previous steps using the appropriate frequency response data. Unfortunately, experimental data for a tire undergoing cyclic lateral displacement are not presently available. In the absence of such data, the theoretical frequency response curves of Ref. 6 can be utilized to develop the necessary expressions.

These theoretical curves are shown in Fig. 6 along with their polynomial approximations. It must be noted, however, that the frequency response functions given here relate the cornering force and aligning torque to the tire slip angle and not to the tire lateral displacement, i.e.,

$$G_{M\alpha}{}^*(j\omega) = [1/G_{M\alpha}(0)][\bar{M}(j\omega)/\bar{\alpha}(j\omega)] \quad (13)$$

$$G_{F\alpha}{}^*(j\omega) = [1/G_{F\alpha}(0)][\bar{F}(j\omega)/\bar{\alpha}(j\omega)] \quad (14)$$

However, from Fig. 1c, we have the kinematic relation

$$\alpha + \psi = y' \quad (15)$$

Taking the Laplace transform under zero initial conditions and noting that for pure sideslip the yaw angle ψ is zero, we obtain

$$\bar{\alpha}(s) = s\bar{y}(s) \quad (16)$$

This relation allows the response functions in Eqs. (13) and (14) to be written in terms of lateral displacement.

By following procedures identical to those used previously for yaw angle inputs, and making use of Eq. (16), one obtains the following frequency response functions for lateral displacement:

$$G_{My}(j\omega) = (j\omega)G_{M\alpha}(0)G_{M\alpha}{}^*(j\omega) = (j\omega)G_{M\alpha}(0)/(1 + j\omega/\omega_5)(1 + j\omega/\omega_6) \quad (17)$$

$$G_{Fy}(j\omega) = (j\omega)G_{F\alpha}(0)G_{F\alpha}{}^*(j\omega) = (j\omega)G_{F\alpha}(0) \times (1 + j\omega/\omega_7)/[1 + (2b_3/\omega_8)j\omega + (j\omega/\omega_8)^2] \quad (18)$$

The corresponding transfer functions are

$$G_{My}(s) = G_{M\alpha}(0)s/(1 + s/\omega_5)(1 + s/\omega_6) \quad (19)$$

$$G_{Fy}(s) = G_{Fy}(0)s(1 + s/\omega_7)/[1 + (2b_3/\omega_8)s + (s/\omega_8)^2] \quad (20)$$

It has been pointed out earlier that under conditions of quasi-steady-state rolling, the cornering force and aligning torque responses to pure sideslip and pure yaw are identical. Therefore, the following identities exist between the frequency response functions at zero frequency:

$$G_{M\alpha}(0) \equiv G_{M\psi}(0) \quad (21)$$

$$G_{F\alpha}(0) \equiv G_{F\psi}(0) \quad (22)$$

Having determined the transfer functions for the individual inputs, the total tire response due to combined motion is now obtained by superposition

$$\bar{M}(s) = G_{M\psi}(s)\bar{\psi}(s) + G_{My}(s)\bar{y}(s) \quad (23)$$

$$\bar{F}(s) = G_{F\psi}(s)\bar{\psi}(s) + G_{Fy}(s)\bar{y}(s) \quad (24)$$

The previous equations of course are restricted to the linear region of tire behavior. This is characterized by small values of slip angle, on the order of $\pm 3°$. Substituting for the transfer functions in Eqs. (23) and (24) yields

$$\bar{M}(s) = G_{M\psi}(0)\{[1 + (2b_1/\omega_2)s + (s/\omega_2)^2]/(1 + s/\omega_1) \times (1 + s/\omega_3)\}\bar{\psi}(s) + G_{M\alpha}(0)\{s/(1 + s/\omega_5)(1 + s/\omega_6)\}\bar{y}(s) \quad (25)$$

$$\bar{F}(s) = G_{F\psi}(0)\{1/[1 + (2b_2/\omega_4)s + (s/\omega_4)^2]\}\bar{\psi}(s) + G_{F\alpha}(0)\{s[1 + (s/\omega_7)]/[1 + (2b_3/\omega_8)s + (s/\omega_8)^2]\}\bar{y}(s) \quad (26)$$

The differential equations corresponding to Eqs. (25) and (26) are obtained directly by first clearing fractions and then taking the inverse Laplace transform of both sides. Obviously, this will result in a fourth-order system in both M and F. It is possible however, at this point, to introduce an approximation which reduces the resulting differential equations to second order. This is achieved by equating the denominators of the fractions in Eqs. (25) and then in Eq. (26), from which we obtain the following necessary relations:

$$\omega_1 + \omega_3 = \omega_5 + \omega_6, \quad \omega_1\omega_3 = \omega_5\omega_6$$
$$b_2 = b_3, \quad \omega_4 = \omega_8 \quad (27)$$

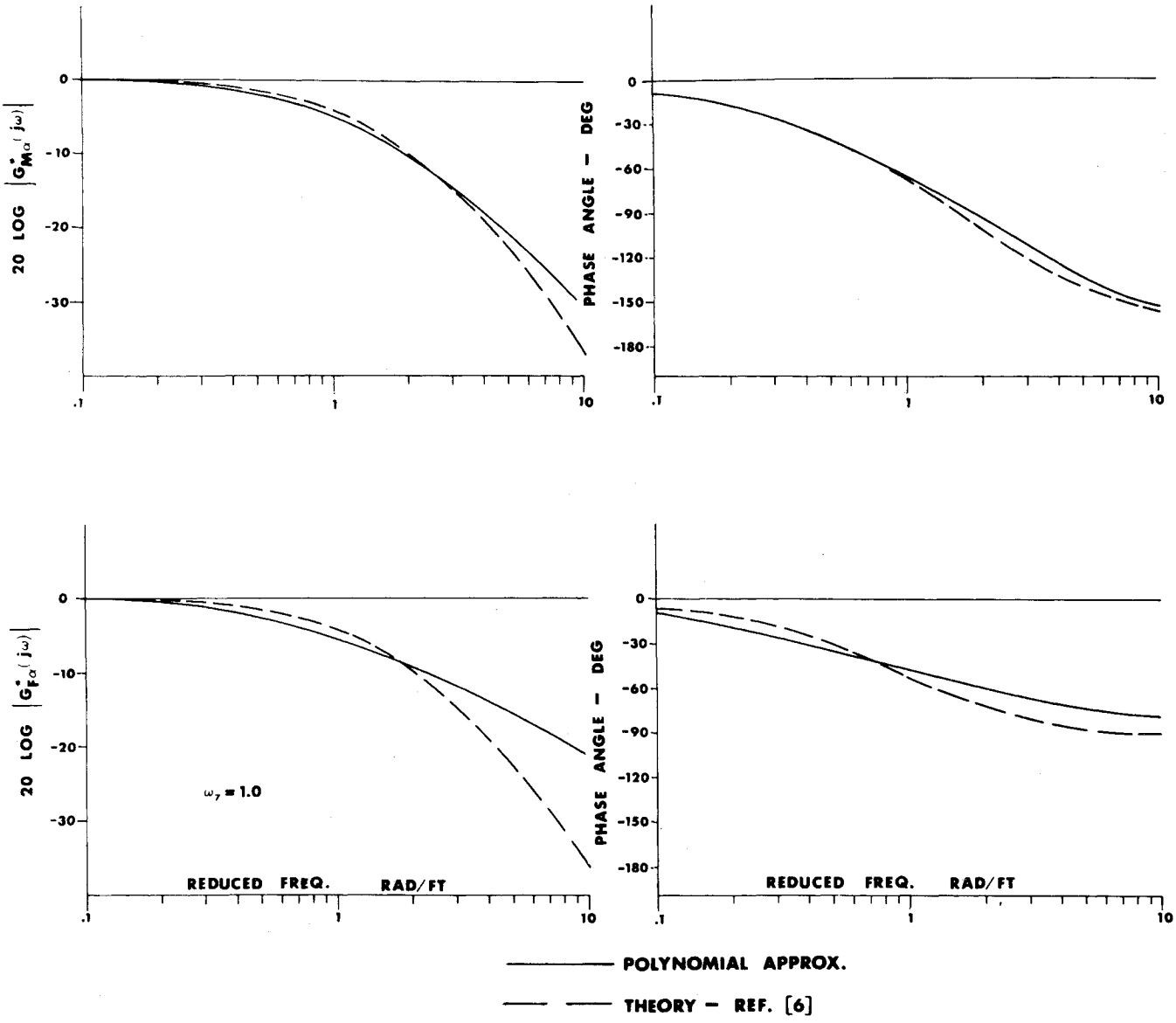

Fig. 6 Tire cornering force and aligning torque frequency response under cyclic lateral displacement.

The approximation is justified on two counts: First, even with the constraints introduced by Eqs. (27), the polynomial approximation of the frequency response curves as displayed in Figs. 3, 4, and 6 was found to be quite good. Secondly, since the theoretical response curves for lateral displacement[6] are based on the tensioned string tire model which is governed by differential equations of the second order, second-order equations would be expected. It should be noted however, that the approximations (27) are in no way essential to the techniques being presented here. Obviously, if more latitude is required in characterizing the tire response, it is easily achieved by omitting Eqs. (27) and resorting to the fourth-order system. Utilizing the approximations given previously, the final differential equations can now be written as follows:

$$M + \left(\frac{1}{\omega_1} + \frac{1}{\omega_3}\right) M' + \frac{1}{\omega_1\omega_3} M'' = G_{M\psi}(0)\left[\psi + \frac{2b_1}{\omega_2}\psi' + \frac{\psi''}{\omega_2{}^2}\right] + G_{M\alpha}(0)y' \quad (28)$$

$$F + \frac{2b_2}{\omega_4} F' + \frac{F''}{\omega_4{}^2} = G_{F\psi}(0)\psi + G_{F\alpha}(0)\left[y' + \frac{y''}{\omega_7}\right] \quad (29)$$

It is preferable for purposes of dynamical analysis to regard the time t rather than the position coordinate x as the independent variable in these equations. The transformation is easily accomplished since for constant forward velocity

$$x = V_x t, \quad d/dx = (1/V_x)(d/dt) \text{ etc.}$$

Thus, written in the time domain, Eqs. (28) and (29) become

$$M + \left(\frac{1}{\omega_1} + \frac{1}{\omega_3}\right)\frac{\dot{M}}{V_x} + \frac{\ddot{M}}{\omega_1\omega_3 V_x{}^2} = G_{M\psi}(0)\left[\psi + \frac{2b_1}{\omega_2 V_x}\dot{\psi} + \frac{\ddot{\psi}}{(\omega_2 V_x)^2}\right] + G_{M\alpha}(0)\frac{\dot{y}}{V_x} \quad (30)$$

$$F + \frac{2b_2}{\omega_4}\frac{\dot{F}}{V_x} + \frac{\ddot{F}}{(\omega_4 V_x)^2} = G_{F\psi}(0)\psi + \frac{G_{F\alpha}(0)}{V_x}\left[\dot{y} + \frac{\ddot{y}}{\omega_7 V_x}\right] \quad (31)$$

where dots denote derivatives with respect to time. These equations contain a total of nine independent parameters of which all but ω_7 are determined from experimental frequency response data for tires undergoing cyclic yaw. At present, such tests can be performed only for smaller size aircraft tires using the equipment described earlier.[9] However, the

U.S. Air Force will soon put into operation an experimental facility which will be capable of measuring the frequency response under yaw for a complete range of aircraft tire sizes and loads.[12] The parameter ω_7 must, for the present at least, be determined from purely theoretical frequency response curves.

Conclusions

Equations (30) and (31) represent a notable improvement over present methods for calculating transient tire forces. They have the advantage of being more accurate than existing tire theories while at the same time retaining a relatively simple form. As explained earlier in this paper, the equations are derived from tire frequency response data. However, they are valid for arbitrary motions of the wheel, provided that the limitation of small slip angles is not exceeded. Another notable feature of this characterization is that higher-order effects such as the influence of camber and wheel speed can be directly accounted for by including them in the test conditions for the frequency response data. The inclusion of such effects by means of tire mechanics theory is presently impractical. Finally, the authors wish to note that this characterization of tire forces is currently being used to great advantage in the study of aircraft single nose-wheel shimmy phenomena.

Appendix

One of the most widely used theories for calculating tire forces in shimmy analysis is that first proposed by Moreland[1] and later elaborated upon by Collins and Black.[10] This theory was developed at a time when it was recognized that the delay properties of tires were an important part of the over-all shimmy phenomena. Although the Moreland tire theory itself has never been subjected to rigorous experimental verification, it has nevertheless provided many useful engineering results. Its continued popularity is due in part to the ease with which it can be incorporated into the equations of motion of the landing gear system. Like the technique described in the body of this paper, the Moreland theory leads to a system of linear, constant coefficient, differential equations. Thus, the transfer functions are readily calculated in terms of ratios of polynomials in s. A comparison of these transfer functions with those derived from experimental data by Bode analysis provide the basis for assessing the validity of Moreland theory.

The extended Moreland tire model can be represented by the mechanical system shown in Fig. 7. It consists of a rigid frame which carries a small, massless, rigid wheel. This wheel is attached to the frame by means of a linear spring k_l and damper C_l. It is also restrained from rotating by the torsional spring k_t. The frame in this model represents the actual tire wheel while the movement of the small rigid wheel corresponds to the motion of the center of the contact patch in the rolling tire. The relative displacement y_1 and rotation α_1 of this fictitious wheel gives rise to the tire force and moment

$$F = k_l y_1 + C_l \dot{y}_1 \tag{A1}$$

$$M = k_t \alpha_1 \tag{A2}$$

In addition, the hypothesis is made that the cornering force is also related to the relative rotation α_1 according to the equation

$$C_y F = -(\alpha_1 + C_1 \dot{\alpha}_1) \tag{A3}$$

In this equation, C_y is the tire yaw coefficient and C_1 is the tire time constant which accounts for the lag between F and α_1. The negative sign indicates that a force F acting in the positive y_1 direction generates a negative or counter clockwise rotation α_1. Finally one additional equation must be

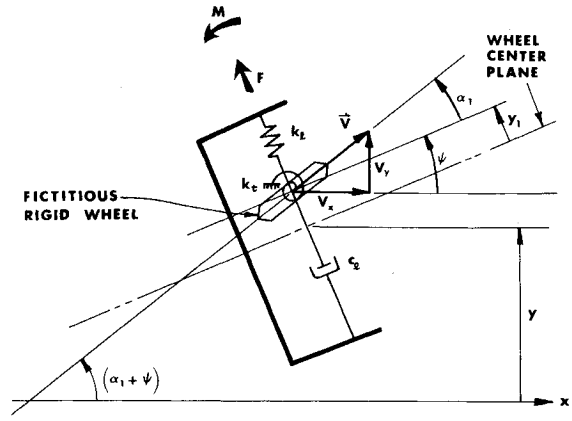

Fig. 7 Moreland tire model.

introduced which relates the wheel coordinates ψ and y to the displacement y_1 and rotation α_1. This is obtained by assuming that the fictitious rigid wheel rolls without sliding in the ground plane, i.e., the instantaneous velocity vector **V** of the rigid wheel is always coincident with its plane. Thus, from Fig. 7, we have

$$\tan(\alpha_1 + \psi) = V_y/V_x \tag{A4}$$

Introducing the assumption of small angles and expressing V_y in terms of y and y_1, one obtains

$$V_x(\alpha_1 + \psi) = \dot{y} + \dot{y}_1 \tag{A5}$$

In order to compare the transfer functions it is necessary to transform the independent variable in Eqs. (A1–A5) from time to the position coordinate x. Making this substitution and then taking the Laplace transform of Eqs. (A1), (A2), (A3), and (A5) under zero initial conditions results in

$$\bar{F}(s) = (k_l + C_l V_x s)\bar{y}_1(s) \tag{A6}$$

$$\bar{M}(s) = k_t \bar{\alpha}_1(s) \tag{A7}$$

$$C_y \bar{F}(s) = -(1 + C_1 V_x s)\bar{\alpha}_1(s) \tag{A8}$$

$$\bar{\alpha}_1(s) + \bar{\psi}(s) = s\bar{y}(s) + s\bar{y}_1(s) \tag{A9}$$

The cornering force response is obtained from Eq. (A9) by substituting for $\bar{y}_1(s)$ and $\bar{\alpha}_1(s)$ from Eqs. (A6) and (A8), respectively.

$$\bar{F}(s) = \{[(k_l + C_l V_x s)(1 + C_1 V_x s)]/ [s(1 + C_1 V_x s) + C_y(k_l + C_l V_x s)]\}[\bar{\psi}(s) - s\bar{y}(s)] \tag{A10}$$

The aligning torque response is obtained by first eliminating $\bar{\alpha}_1(s)$ between Eqs. (A7) and (A8) and then substituting for $\bar{F}(s)$ from Eq. (A10).

$$\bar{M}(s) = -k_t C_y\{[k_l + C_l V_x s]/[s(1 + C_1 V_x s) + C_y(k_l + C_l V_x s)]\}(\bar{\psi}(s) - s\bar{y}(s)) \tag{A11}$$

The frequency response functions can be written directly from Eqs. (A10) and (A11) as follows:

$$G_{F\psi}(j\omega) = 1/C_y((1 + (C_l V_x/k_l)j\omega)(1 + C_1 V_x j\omega)/ \{1 + [(C_y C_l V_x + 1)/C_y k_l]j\omega + (C_1 V_x/C_y k_l)(j\omega)^2\}) \tag{A12}$$

$$G_{Fy}(j\omega) = -(j\omega)G_{F\psi}(j\omega) \tag{A13}$$

$$G_{M\psi}(j\omega) = -k_t((1 + (C_l V_x/k_l)j\omega)/ \{1 + [(C_y C_l V_x + 1)/C_y k_l]j\omega + (C_1 V_x/C_y k_l)(j\omega)^2\}) \tag{A14}$$

$$G_{My}(j\omega) = -(j\omega)G_{M\psi}(j\omega) \tag{A15}$$

It follows also from Eq. (16) that the frequency response functions $G_{F\alpha}(j\omega)$ and $G_{M\alpha}(j\omega)$ will be given by

$$G_{F\alpha}(j\omega) = -G_{F\psi}(j\omega) \tag{A16}$$

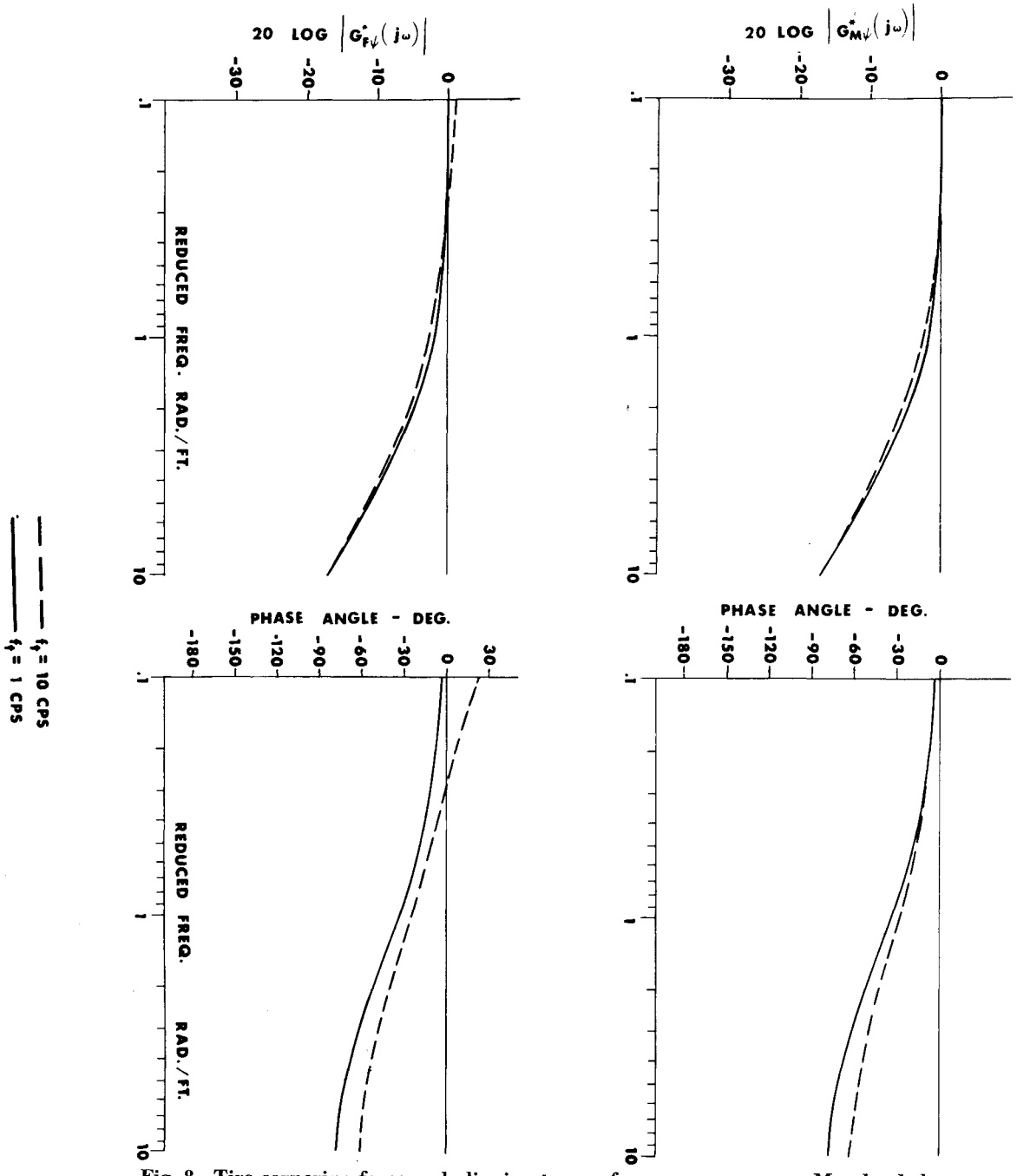

Fig. 8 Tire cornering force and aligning torque frequency response—Moreland theory.

$$G_{M\alpha}(j\omega) = -G_{M\psi}(j\omega) \tag{A17}$$

Thus, it is seen that the frequency response for sideslip is identical to that for yaw except for sign. Upon normalizing by the response at zero frequency, we have

$$G_{F\alpha}{}^*(j\omega) = G_{F\psi}{}^*(j\omega) \tag{A18}$$

$$G_{M\alpha}{}^*(j\omega) = G_{M\psi}{}^*(j\omega) \tag{A19}$$

This result is in disagreement with that obtained in Refs. 3, 4, and 6 where it was found that frequency because of the yaw and sideslip were notably different except for the special case of zero reduced frequency. Moreover, a comparison of the frequency response functions $G_{F\psi}(j\omega)$ and $G_{M\psi}(j\omega)$ given here with those derived by Bode analysis reveal certain important differences in form. For example, both Eqs. (10) and (A10) have second degree terms in the denominator, but the numerator consists of a constant and a product of two first degree terms, respectively. Similar differences exist between Eqs. (9) and (A12). Unfortunately because of the present lack of data, the frequency response functions derived from Moreland theory cannot be directly compared with experimental results for a particular tire. However, the form of the response curves can be illustrated for a typical nose-wheel aircraft tire by making use of the tire parameters given by Collins in Ref. 11. Figure 8 shows the normalized frequency response curves based on the following tire data for an 18 × 5.5 tire loaded to 3100 lb: $k_l = 1.938 \times 10^4$ lb/ft, $C_y = 7.5 \times 10^{-5}$ rad/lb, $C_l = 1.068 \times 10^2$ lb-sec/ft, $k_t = 3.31 \times 10^3$ ft-lb/rad, and $C_1 = 1.32 \times 10^{-5}(V_x)$ sec/rad. Notice that the time constant C_1 is given as a linear

function of the forward velocity V_x. This velocity dependence was determined experimentally in Ref. 10 and is considered essential to a proper description of the tire using Moreland theory.

References

[1] Moreland, W. J., "Landing-Gear Vibration," AF TR 6590, 1951, Wright-Patterson Air Force Base, Dayton, Ohio.

[2] von Schlippe, B. and Dietrick, R., "Das Flattern eines bepneuten Rades," Teil A: Zur Pneumechanik, Bericht der Lilienthalgesellschaft für Luftfahrtforschung Nr. 140, 1941, S.35-41, Berlin; also TM 1365, 1954, NACA.

[3] Segel, L., "Lateral Mechanical Characteristics of Non-Stationary Pneumatic Tires," Rept. YD-1059-F-1, April 1956, Cornell Aeronautical Laboratory, Buffalo, N.Y.

[4] Saito, Y., "A Study of the Dynamic Steering Properties of Pneumatic Tyres," Ninth International Automobile Technical Congress, Fédération International des Sociétés D' Ingénieurs des Techniques De L'Automobile (FISITA), Paris 1962.

[5] Smiley, R. F., "Correlation, Evaluation, and Extension of Linearized Theories for Tire Motion and Wheel Shimmy," Rept. 1299, 1957, NACA.

[6] Pacejka, H. B., "The Wheel Shimmy Phenomenon," Ph.D. thesis, Delft Technical Institute, Delft, The Netherlands, 1966.

[7] D'Azzo, J. J. and Houpis, C. H., "Feedback Control System Analysis and Synthesis," 2nd Ed., McGraw-Hill, New York, 1966, pp. 175–94.

[8] Brewer, H. K., "Cornering Force and Self-Aligning Torque Response of a Tire Undergoing Sinusoidal Variations in Steer Angle," Rept., B. F. Goodrich Research Center, Nov. 1965, Brecksville, Ohio.

[9] Ginn, J. L. et al., "The B. F. Goodrich Tire Dynamics Machine," *SAE Journal*, Vol. 70, July 1962, p. 88; also SAE Paper No. 490B.

[10] Collins, R. L. and Black, R. J., 'Tire Parameters for Landing-Gear Shimmy Studies," *Journal of Aircraft*, Vol. 6, No. 3, May-June 1969, p. 252.

[11] Collins, R. L., "Theories on the Mechanics of Tires and Their Application to Shimmy Analysis," *Journal of Aircraft*, Vol. 8, No. 4, April 1971, pp. 271–277.

[12] Sperry, G. J., "New Generation of Aircraft Tire Test Dynamometers," *19th DOD Nondestructive Testing Conference*, No. 4, 1970, St. Louis, Mo.; also proceedings to be published by U.S. Army Mobility Equipment Command, St. Louis, Mo.

[13] Attri, N. S and Domandl, H, "Impact of Tire Dynamic Properties on Airplane Landing-Gear Shimmy," SAE A-5 Committee Meeting Minutes, Oct. 14, 1970, San Diego, Calif.